Article

Artificial Intelligence Enabled Radio Propagation: Path Loss Improvement and Channel Characterization in Vegetated Environments

Leonardo Gonsioroski[1], Amanda Santos[1], Jairon Viana[1], Sandra Ferreira[1], Rogerio Silva[1]
Luiz da Silva Mello[2], Leni Matos[3], Marcelo Molina[4]
[1]Universidade Estadual do Maranhão, São Luís, Brasil, gonsioroski@uema.br, amandabiacs@gmail.com, engenharia.pl06@gmail.com, sandraeloi07@gmail.com, rogeriomls@uema.br
[2]Pontificia Universidade Católica do Rio de Janeiro, Rio de Janeiro, Brasil, larsmello@cetuc.puc-rio.br
[3]Universidade Federal Fluminense, Niterói, Brasil, lenijm@id.uff.br
[4] Ingeniería de Telecomunicaciones Universidad Católica Boliviana "San Pablo", La Paz, Bolívia, mmolina@ucb.edu.bo

***Abstract* — In this paper, the application of AI and machine learning (ML) to the study of wireless propagation channels is investigated in two parts: first, an artificial neural network model is used to improve path loss prediction, and then, a pattern recognition model using multilayer perceptron (MLP) networks is used to identify and remove impulsive noise in power delay profiles (PDP). These studies were conducted based on field measurements in the 2400 MHz band in a public square with vegetation. The results are analyzed and compared with ordinary least squares (OLS) nonlinear regression results and results from similar studies. The Root Mean Square Error (RMSE) values between the experimental results of mean path loss and those provided by each propagation model are presented. The adjustment performed by OLS nonlinear regression and ANN significantly reduced the RMSE. The best results are those presented by artificial neural networks, with RMSE of 0.39 when using four neurons in the hidden layer of the ANN. The ANN used to identify and remove impulsive noise in power delay profiles (PDP) through pattern recognition proved to be more efficient than the CFAR technique. ANN technique found a larger number of valid multipaths compared to the CFAR technique.**

***Index Terms*—**Artificial neural network, machine learning, path loss, propagation in vegetation.

I. INTRODUCTION

Radiofrequency communications have undoubtedly reached the top of the hierarchy of importance in telecommunications services. In the upcoming years, a remarkable revolution is poised to transform various sectors of the global economy. Two new standards will be responsible for this revolution in this huge market: the fifth generation (5G) of mobile communications and the sixth generation of WLAN (IEEE 802.11ax). The new IEEE 802.11ax standard [1] was designed for high-density environments like trains, stadiums, and airports. Moreover, this technology is expected to bring advantages to Internet

received 15 Aug 2023; for review 27 Sep 2023; accepted 31 Jan 2024

ISSN 2179-1074

of Things (IoT) implementations and home and office networks, with considerably lower deployment costs compared to 5G. Its operation will occur in the unlicensed bands of 2.4 and 5 GHz. The 5G will operate in low and medium frequencies and mm Waves, with sub-6GHz bands being the most recommended in its initial implementation stage [2]. In Brazil, the National Telecommunications Agency (ANATEL - Agência Nacional de Telecomunicações) decided that 5G will initially operate in the bands between 2300-2400 MHz (n40) and 3300-3800 MHz (n78). These frequency bands balance wide coverage area and high capacity, economical implementation, and greater penetration into internal environments.

Accompanying this evolution and popularization of mobile networks, the public administration of states and municipalities in Brazil has invested in the adoption of internet access points for free use in public spaces of great circulation, such as squares, parks and bus stations, promoting digital and social inclusion, improving the experience of visitors in the practice of ecotourism in Conservation Units. There are also programs aimed at communities in a state of social vulnerability and environmental conservation areas. Both the environmental conservation units and most public squares and parks in Brazil are environments predominantly covered by vegetation, which directly impacts the propagation of electromagnetic waves in these areas. Therefore, several research works [3]-[10] on the behavior of electromagnetic waves in environments with a large presence of vegetation for various applications have been carried out in recent decades.

Several models [11]-[16] were developed to estimate the propagation loss in vegetated environments. However, they are specific and not applied in all scenarios. Therefore, it is important for the modeling based on empirical data and the improvement of the existing models.

On the other hand, Artificial Intelligence (AI) techniques have rapidly advanced in many domains since the last decade, including Radio Propagation. AI allows the system to correctly interpret external data, learn from such data, and use those learnings to achieve specific goals and tasks through flexible adaptation [17]. Machine learning (ML) is a branch of AI that enables machines to learn from a massive amount of data. ML techniques have also been widely applied in various propagation channel research [18]-[19]. In this context, we investigate the application of AI to the study of wireless propagation channels in vegetated environments. ML techniques in propagation loss improvement, using artificial neural network (ANN) in the nonlinear regression of field measurement data, and in wideband channel characterization, in particular, in the filtering technique (CFAR), are used for mitigating the effect of impulsive noise in power delay profiles (PDP). This procedure guarantees a more assertive determination of the time dispersion parameters of the channel.

Experimental results of time dispersion and coverage statistics of an outdoor reception signal in the 2400 MHz band, focusing on the electromagnetic coverage of a public park with vegetation between the transmitter and the receiver, will be presented. Narrowband and wideband characterizations are performed by processing data obtained with a continuous wave (CW) signal and orthogonal frequency division multiplexing (OFDM) with a bandwidth of 20 MHz, respectively. Statistical results for the path loss exponent are presented. From the relation of the propagation loss of the received signal with the distance, comparisons of adherence were made with some propagation models already established in the literature.

The remainder of the paper is organized as follows. Section II presents previous related works concerning the characterization of the channel in vegetated environments and the application of ML techniques in radio propagation. Section III discusses the narrowband and wideband sounding techniques used in this paper. Section IV summarizes the main empirical path loss models for vegetation environments. Section V introduces how AI techniques will improve propagation loss prediction and delay profile filtering. Section VI details the measurement environment and setup. Sections VII discuss the results. Section VIII concludes the paper.

II. Related Works

The study of the behavior of the electromagnetic wave propagated in an environment with the presence of vegetation was carried out in many different scenarios and different frequency bands. Adewumi and Olabisi [7] investigated the propagation behavior of radio waves in the 1,835 MHz band along a long-forested channel of about 8 km with mixed vegetation of different densities. The results showed that the generic models, mainly modified exponential decay, provided significant errors for the long forest channel scenario, and the authors proposed a new model. Leite et al. [8] characterized the radio frequency channel in a propagation environment with particular vegetation and a lake. The authors identified the communication channel model that best describes communication characteristics; the effects of large-scale fading, such as path loss and log-normal shadowing; the characterization of small-scale fading (multipath and Doppler) and the estimation of the aircraft speed from the identified Doppler frequency. Azpilicueta et al. [9] characterized radio channels for wireless sensor networks (WSNs) ISM 2.4 GHz in an environment of non-homogeneous vegetation. The analysis allows the design of ZigBee and WiFi-based environment monitoring tools where WSN and smartphones cooperate, providing rich and personalized monitoring information to users in a user-friendly way. Pires et al. [10] carried out the broadband characterization of the mobile radio channel in environments with vegetation in the 2.5 GHz band. In those studies, the authors positioned the transmitting antenna at an altitude of tens of meters, equivalent to the height of 4G base stations. Measurements were carried out kilometers away from the transmitter.

In this paper, the measurement, modeling, and validation of existing models on the effect of vegetation in a common square, typical in Brazil, are reported. This investigation is distinguished from the others by considering the transmission antenna at only 3 meters high, typically the height of transmitters in this type of scenario.

As mentioned in the introduction, many investigations of radio channel propagation involving

Machine Learning techniques have been carried out in recent years. Some of these are aimed at coverage analysis and channel characterization.

Some papers [20]-[23] applying ML to propagation channels studies have been published, where the coverage prediction modeling of propagation signal is the focus of the studies. Zhang et al [20], present the principles and procedures of machine learning-based path loss prediction evaluating the performance of different models such as artificial neural network, support vector regression, and random forest. Authors show that these machine-learning-based models produces excellent results. Sotiroudis et al. [21] make use of Convolutional Neural Network (CNN) to improve path loss prediction. The results found are satisfactory and the authors propose the application of the methodology for path loss prediction in urban environments for several state-of-art wireless networks like 5G and Internet of Things (IoT). Shin Jo et al. [22], proposes a machine learning framework for modeling path loss using a combination of three key techniques: artificial neural network (ANN)-based multi-dimensional regression, Gaussian process-based variance analysis, and principal component analysis (PCA)-aided feature selection. ANN then learns the path loss structure from the dataset with reduced dimension, and Gaussian process learns the shadowing effect. The authors show that the combined path loss and shadowing model is more accurate and flexible compared to the conventional linear path loss plus log-normal shadowing model. Moraitis et al. [23] assesses various machine learning methods that aim at predicting path loss in rural environment. The results demonstrate that all the proposed machine learning models outperform the empirical ones, exhibiting, in any case, root-mean-square-error (RMSE) values between 4.0 and 6.5 dB.

However, few studies have been performed in applying artificial neural networks to identify multipath in power delay profiles [24]. In this research, ANNs were used to identify valid multiple paths in power delay profiles obtained from the impulse response of the outdoor channel in the 2400 MHz band with vegetation.

III. Channel Characterization and Sounding Technique

A transmitted radio signal reaches the receiving mobile station by three main propagation mechanisms: reflection, diffraction, and scattering. Furthermore, the envelope and phase of the received signal vary randomly because electromagnetic waves travel along different paths of varying lengths, called multipath. Because of this randomness, the mobile propagation radio channel is studied and analyzed statistically.

Incident energy absorption, signal scattering, dispersion, and depolarization are important in vegetation propagation. Hence, understanding the statistical behavior of electromagnetic waves propagated in channels with vegetation presence becomes crucial. This statistical behavior can be analyzed from a narrowband channel sounding perspective and a wideband channel sounding.

  ISSN 2179-1074

A. Narrowband Channel Sounding

In the narrowband sounding, it is possible to evaluate the behavior of the received signal power as the receiver moves around the transmitter and thus evaluate propagation loss in a given environment. Several models already established in the literature are often used to predict propagation losses in environments with vegetation. Still, these models cannot always correctly express the real losses in all types of scenarios, which leads to the need to develop specific models for specific scenarios. Furthermore, the multipath effect generates small-scale variability and echoes at the receiver caused by the arrival of replicas delayed with respect to the first component of the received signal, causing time and frequency dispersion. Small-scale variability can be investigated through field measurement campaigns using narrowband channel sounding techniques, where a narrowband signal (CW) is used as a test signal.

B. Wideband Channel Sounding

Wideband channel sounding allows us to obtain channel impulse response (CIR) and know the power delay profiles (PDP) through it. The PDP will allow us to identify the replicas of the signal that reach the receiver and thus obtain channel dispersion parameters in the time and frequency domains. In this paper, we will focus our analysis on the time dispersion of the channel.

There are numerous wideband sounding techniques for characterization in indoor and outdoor environments. among the most representative, known in the literature, is the transmission technique of a train of periodic narrow pulses [25], the pulse compression technique [25], and the transmission technique of signals with multiple carriers based on OFDM [26]-[27]. The OFDM is a multiport technique that is easy to implement. It does not require cables for synchronization between Tx and Rx, making it ideal for outdoor soundings and immunity to multipath fading and impulsive noise [28].

In the multicarrier sounding technique, an OFDM symbol with a cyclic prefix is generated and transmitted sequentially on the channel. A gap is inserted between transmitted symbols. The signal captured by the receiving antenna is stored. A cross-correlation process between the received signal and the originally generated OFDM symbol allows the identification of each received OFDM symbol [25]. As shown in Fig. 1, the OFDM symbols are identified by the gap introduced and by the correlation peaks caused by the cyclic prefix and the ODFM symbol during the cross-correlation process.

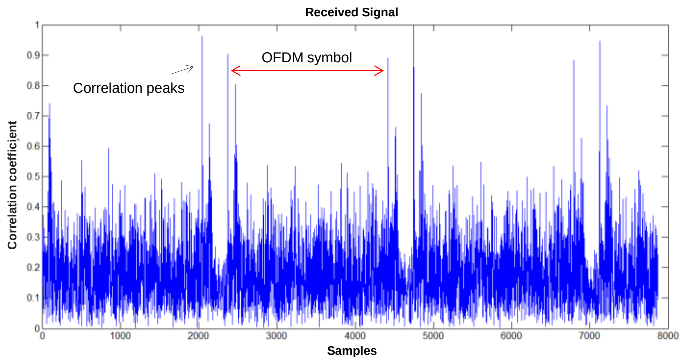

Fig. 1. Transmission and reception setups for narrowband and wideband sounding.

  ISSN 2179-1074

Narrowband channel sounding and wideband channel sounding schemes can be seen in [29]. The OFDM sequence and PN signal parameters are presented in Table I.

Table I. configuration of the ofdm signal

Parameter	Value	Measurement unit
Channel bandwidth [BW]	20	MHz
FFT size [NFFT]	1024	Samples
Sampling factor	2	-
Sampling rate	50.10^6	Samples/second
Number of used carriers [N_{used}]	800	Carriers
PN length	1023	bits
Cyclic Prefix [CP]	1/16	Samples

In this paper, we will apply the scheme that combines the advantages of the multicarrier techniques and STDCC was proposed and employed by [30], in which a PN signal is OFDM modulated and transmitted over the communication channel. Thus, the power delay profile is directly obtained by the cross-correlation between the received signal and a copy of the transmitted signal.

IV. Empirical Path Loss Model in Vegetation Environment

The vegetation attenuation models can be classified into empirical and analytical ones. Empirical vegetation attenuation models developed using experimental data are convenient for their simplicity, even though this method overlooks the measurement's geometry and fails to differentiate between various modes of propagation. The Modified Exponential Decay (MED) and the Maximum Attenuation (MA) are widely used generic empirical models. Both approaches assume that path loss in vegetation increases exponentially with distance.

A. Modified Exponential Decay (MED) Models

The Modified Exponential Decay modeling considers different parameters for different types of vegetation and frequency ranges, whose mathematical expression is given by:

$$L_{vegetation} = a * f^b * d^c \tag{1}$$

and α, b and c were determined from empirical measurements considering different environments and frequency ranges.

The first MED-type model was proposed by Weissberger [11] in 1982. Weissberger's model was developed in the situation where both antennas were in the ground with a foliage depth of 400 m and a frequency range of 230 MHz to 95 GHz, applicable in situations where propagation occurs through the grove of trees. About 1988, The International Telecommunication Union (ITU) developed a propagation loss model for vegetated paths using Weissberger's same technique and frequency range. This model is known as the Early ITU-R model [12]. Just like Weissberger's model, the Early ITU-R model is applicable in areas with a high density of vegetation, and which have a presence of geometry in which the transmitting or receiving antenna is near enough to a small (less than 400 m deep) grove of trees so that the majority of the signal propagates through the trees. To get a more generic model, the European Co-operation in Science and Technology (COST) developed another model called COST 235

Brazilian Microwave and Optoelectronics Society-SBMO received 15 Aug 2023; for review 27 Sep 2023; accepted 31 Jan 2024
Brazilian Society of Electromagnetism-SBMag *ISSN 2179-1074*

[13] in 1996. This model was developed using measurements conducted on 9.6 GHz and 57.6 GHz frequencies.

In 1998, Al-Nuaimi et al. [14] proposed a new model known as Fitted ITU-R. The Fitted ITU-R gives the excess attenuation as a function of vegetation depth and frequency and is recommended for use at frequencies of 10 to 40 GHz, considering in-leaf and out-of-leaf vegetation scenarios.

B. Maximum Attenuation (MA) Model

The maximum attenuation model (ITU-R 833-6) [15] is recommended by International Telecommunications Union (ITU) for a frequency range of 30 MHz–30 GHz. This model considers that the additional loss due to vegetation can be characterized based on two parameters. First, the specific attenuation rate (γ) due primarily to the scattering of energy out of the radio path, as would be measured over a very short path; and second, the maximum total additional attenuation due to vegetation in a radio path (A_m) as limited by the effect of other mechanisms, including surface-wave propagation over the top of the vegetation medium and forward scatter within it. The excess attenuation due to the presence of the vegetation is given by [15]:

$$L_{vegetation} = A_m \left[1\text{-}e^{-\frac{\gamma d}{A_m}}\right] \tag{2}$$

where d is the vegetation depth in meters.

The value of specific attenuation due to vegetation, γ dB/m, depends on the species and density of the vegetation. Approximate values are given in Fig. 2 [15] as a function of frequency for horizontal and vertical polarizations. For the frequency range used in this work, the value of y chosen was 0.45.

The parameter A_m has a frequency dependency of the form:

$$A_m = a \cdot f^b \tag{3}$$

in which f is the frequency (MHz). According to Rec. ITU-R P.833-6 for measurements conducted in Europe for 900-2200 MHz frequency range, a = 1.15 and b = 0.43.

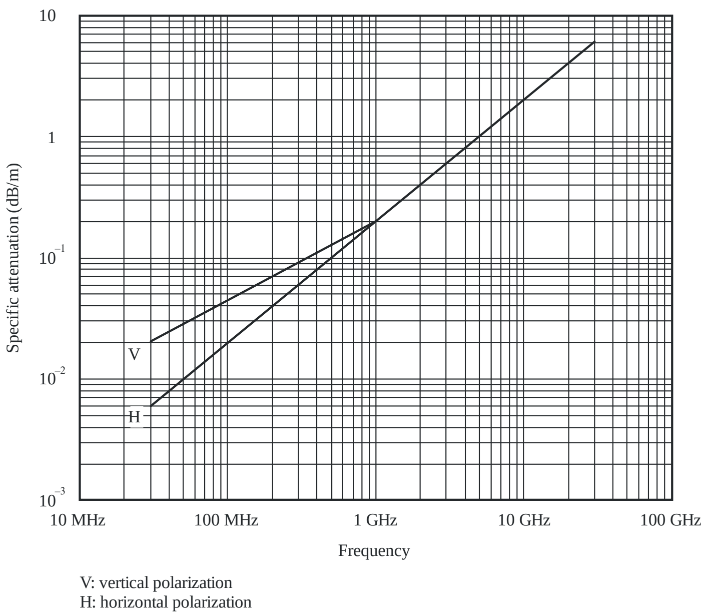

Fig. 2. Specific attenuation due to vegetation, in dB/m, as a function of frequency [15].

In 1998 Al-Nuaimi et al. [14] proposed a new model known as Fitted ITU-R. The Fitted ITU-R gives the excess attenuation as a function of vegetation depth and frequency. It is recommended for use at 10 to 40 GHz frequencies, considering in-leaf and out-of-leaf vegetation scenarios. Parameters a, b and c for Weissberger, the Early ITU, COST-235 and Fitted ITU-R models are presented in Table II.

TABLE II. PARAMETERS OF MODIFIED EXPONENTIAL MODELS

	α	**b**	**c**
Weissberger for $14 \leq d \leq 400m$	1.33	0.284	0.588
Early ITU-R for $d \leq 400m$	0.2	0.3	0.6
COST-235, with leaves	15.6	- 0.009	0.26

C. Chen and Kuo Model

Chen and Kuo [16] addressed the propagation loss in forest environments using measurements in the 1 to 100 GHz band. They have proposed a model based on the Geometric Theory of Diffraction and the medium was modeled by four layers: air, canopy, tree trunks and soil [34]. The expressions are given by [16]:

$$L_{vegetation} = (a \cdot f + b)d + c \cdot f + d \quad (4)$$

where for vertical polarization $\alpha = 0.001$, $b = 0.2$, $c = 0.5$ and $d = 3$; and for horizontal polarization $\alpha = 0.0002$, $b = 0.2$, $c = 0.3$ and $d = 2$.

V. APPLICATION OF ARTIFICIAL NEURAL NETWORKS IN CHANNEL CHARACTERIZATION

Machine learning techniques have been considered excellent tools to analyze the propagation process of electromagnetic waves, as they have powerful resources for learning and prediction based on the data generated in situations of great complexity and bringing them closer to nonlinear systems. Models based on neural networks are suggested as a potential alternative in the modeling of Radio Propagation Channels in digital TV systems, as an improvement of prediction in the ITU models at the UHF Band [22], or as models of prediction of propagation losses in LTE (Long Term Evolution) and LTE-Advanced [31] communication networks. There are numerous variants of neural networks, allowing for architecture customization based on application requirements or the designer's preferences.

Many works have been developed to seek better propagation loss prediction results using some Machine Learning techniques [22], [33-34]. In this work, neural networks are applied to models for predicting the propagation loss of an electromagnetic wave through the nonlinear regression of data obtained from measurement campaigns and were used to identify multipath in power delay profile. In both cases, we will use multilayer perceptron (MLP) networks. MLP networks have shown high potential in solving problems involving a high degree of non-linearity in engineering. In the case of MLP networks, the learning carried out is supervised. In this learning, the neural network receives an input vector and an output vector with the desired result. The network can be trained by adjusting the synaptic weights of each interconnection between neurons to find a connection between the available data. Then, the results are compared with the desired data, and the error information found feeds the neural network to improve its efficiency. Before training, initial weights with small random values are assigned to the synapses. The activation functions defined for each neuron decide whether the information they receive is relevant or should be ignored.

In the ANN, the input data are inserted into a training algorithm that communicates numerical signals by adjusting the weights, generating a stimulus signal that will be incorporated into the route deviation using an activation function. These inputs, often standardized, are characteristic of the data under analysis. For ANN training, MATLAB® software was used to produce an MLP (Multilayer Perceptron) neural network with the aid of the backpropagation training algorithm with a specific tool called the Neural Network Fitting Tool. This simulator was chosen due to its effectiveness, simplicity, and knowable graphical interface.

A. Application of Artificial Neural Networks in Path Loss Prediction

In this work, neural networks are applied to models for predicting the propagation loss of an electromagnetic wave through the nonlinear regression of data obtained from measurement campaigns. The backpropagation algorithm using the descending gradient method is one of the most widely used supervised learning algorithms for multilayer feedforward neural networks. However, in nonlinear regression problems, the algorithm based on descending gradients is very slow, taking a very high number of epochs to converge and reach acceptable minimum error values [35]. Several variations of the backpropagation method have been proposed to make the convergence process more efficient. Then, an efficient way to solve nonlinear regression problems is using the Gauss-Newton algorithm or the Levenberg-Marquardt (LM) algorithm. Both methods allow you to calculate a least-squares solution in nonlinear function regression.

The Levenberg-Marquardt algorithm is an extension of the Gauss-Newton algorithm. Some improvements introduced by Levenberg [36] and Marquardt [37] allowed the algorithm to solve problems involving nonlinear regression functions more efficiently. The LM method is a second-order gradient method, which can be incorporated into the backpropagation algorithm to enhance the efficiency of the training process [38] and is normally used to perform nonlinear regressions where the Gauss-Newton algorithm does not converge [39].

According to [36], in the Levenberg-Marquardt algorithm, the increment of weights Δw can be obtained as follows:

$$\Delta w = [J^T(w)J(w) + \mu I]^{-1} J^T(w) E \tag{5}$$

where $J(w)$ is the Jacobian matrix, $J^T(w)$ is the Hessian matrix, I is the identity matrix, E is the error vector containing the output errors for each input vector used in the network training, and μ is a parameter that adjusts the convergence rate of the Levenberg-Marquardt algorithm. This parameter is adjusted at each iteration and guides the optimization process. Suppose the reduction of error E is occurring quickly. In that case, μ may be a small value, making the Levenberg-Marquardt algorithm

  ISSN 2179-1074

approach the Gauss-Newton algorithm. In contrast, if the iteration gives an insufficient reduction, μ can be increased by taking a step closer to the direction of the gradient's descent [40]. Thus, such a parameter must be large enough to decrease the objective function and approach zero in the algorithm's final stages so that the Gauss-Newton Method's quadratic convergence is recovered.

Compared with many neural network structures, MLP neural network, which is trained by the BP algorithm, is more mature in theory and performance. It has the advantages of simple structure, stable state, and easy implementation, making it ideal for path loss prediction applications. For efficient modeling of propagation loss by the neural network, we sought to organize the input vectors in an optimized way. Several experiments were conducted with numerous configurations of the network's hyperparameters to find the best result, which will be presented in a further section.

B. Application of Artificial Neural Networks as a Filtering Technique

To ensure the good performance of wireless communication systems, it is important to know the characteristics of the communication channel. The sounding techniques are the experimental tools used to know the characteristics of the mobile communication channel.

When sounding a channel and collecting data and information in the receiver, the presence of environment intrinsic noise and the electronic equipment involved in the measurement process are recorded. Therefore, it is common to use post-processing techniques of the collected signals at the time of the measurement to remove or reduce noise in identifying the multipath that reaches the receiver. These techniques are known as PDP filtering techniques because the delays generated by the scattering of the signal can be mistaken in the receiver by impulsive noise, which must be removed from the final analysis of the channel characterization. To distinguish the true multipath from the impulsive noise, it is necessary to perform filtering on the power delay profiles. A technique has been constantly used for this purpose is the CFAR filtering technique [41]. The good results provided by the CFAR technique [45-50] accredit it as a valid technique and widely accepted by the academic community.

The application of the CFAR technique oriented to delay profile filtering is initially based on the determination of a noise threshold for each of the PDPs obtained in the field measurements. This noise threshold is determined according to what is presented in [41]. Then all echoes from each PDP will be analyzed. The CFAR technique assumes that it is statistically unlikely that the large noise samples will be present at the same delay in all three PDP records in sequence. Therefore, a PDP echo is considered a true echo or not an impulsive noise if the two conditions below are met simultaneously: 1. The noise threshold was exceeded both in the analyzed echo and the equivalent echo of the previous and post-PDP and 2. At least one previous or post echo, to the analyzed echo, on the same PDP satisfies item 1.

If these two conditions above are satisfied, the echo is valid. Therefore, the CFAR algorithm proposes that impulsive noise spurs with power above the threshold, which mixes with true echoes, occur randomly and are unlikely to be present in three PDPs measured in sequence. In other words, there is a pattern in the echos that arrive at the receiver in three or more measurements performed in sequence because the reflectors and scatterers in that short period of time are, a priori, the same.

Following this reasoning, in [24], the authors propose an MLP ANN to identify, by pattern recognition, the impulsive noise samples inserted in the PDPs generated from field measurements, considering that the impulsive noise will not follow the same pattern of occurrence of the true echos.

In this paper, we used ANN to identify valid echoes from field measurements for wideband channel characterization. However, we used the vector of results obtained by the CFAR technique as a target vector for the supervised learning of the artificial neural network. ANN was trained from the input of seven information vectors regarding each of the various PDPs, obtained empirically: 1. <u>Threshold</u>: noise threshold determined according to what is presented in [41]; 2. <u>Average</u>: mean values of the power of all PDP echoes before applying the filtering technique; 3. <u>Median</u>: median values of the power of all PDP echoes before applying the filtering technique; 4. <u>Standard deviation</u>: standard deviation values of the power of all PDP echoes before applying the filtering technique; 5. <u>Power</u>: power value of each echo from the PDP under analysis; 6. <u>Predecessor</u>: power values of all echoes from the PDP immediately preceding the PDP under analysis; and 7. Successor: Power values of all echoes of the PDP immediately after the PDP under analysis.

As was mentioned, the CFAR technique is also applied to analyze the same PDPs, and its results are used as the neural network's desired/target output vector. Fig. 3 shows the schema of the neural network generated in the MATLAB® software.

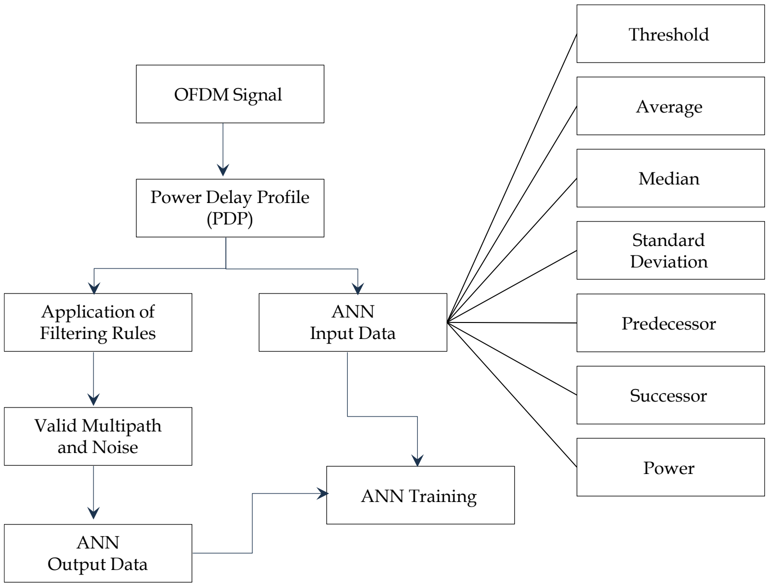

Fig. 3. Stages of ANN input and output preprocessing.

Despite the good results and consistency of the results of the CFAR technique, in [24] the authors note CFAR's inability to resolve multipath components with shorter interarrival time. According to them, the ANN technique found more true echoes than the CFAR technique. The greater identification of true echoes of the ANN technique leads to different values of average excess delay and RMS delay spread obtained using the CFAR and ANN techniques. Although the values have some agreement, it is important to highlight the results of learning and recognition of standards ANN to consider its results more reliable.

VI. Measurements Environment and Equipment Setup

A. Environment

The chosen scenario was the campus of the Pontifical Catholic University of Rio de Janeiro (PUC-Rio) with the presence of vegetation and a certain degree of urbanization. As expected, the university campus is an environment with many dispersers, among them bushes and large trees with much foliage, benches and concrete tables, an area for the circulation of people and cars, and a parking lot, typically representing the desired study environment. Fig. 4 shows three different views of the propagation region of the test signal and a top view of the studied area. The green line shows the route taken during measurements. The purpose of the measurements was to collect empirical data that would allow for channel characterization, including signal variability statistics, path loss, signal coverage, and dispersion parameters for the outdoor-to-outdoor channel. For that, two different measurement setups were installed: one for the narrowband probe and the other for the wideband one.

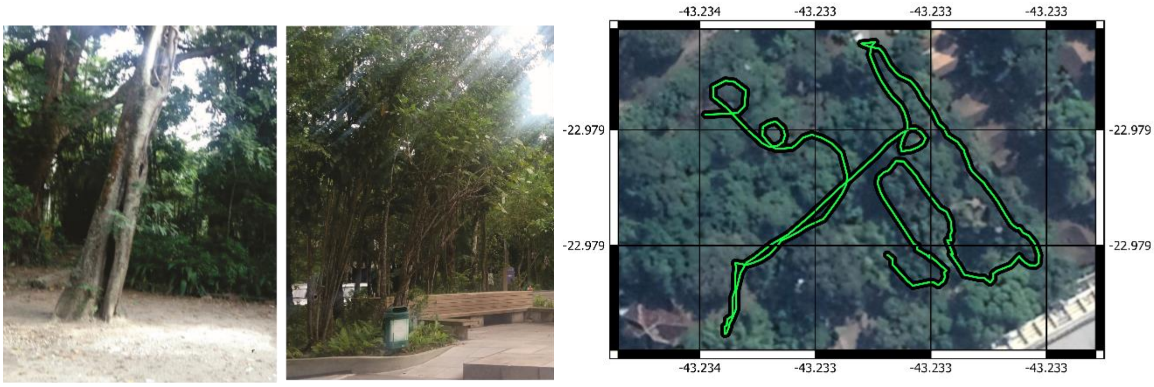

Fig. 4. Measurements Environment.

B. Narrowband Measurements Setup

The narrowband channel sounding is probed by a CW unmodulated 2.4 GHz tone generated by an MG3700A Vector Signal Generator. Its RF output is connected to a power amplifier of 46 dB gain and an omnidirectional antenna with a 3 dBi gain mounted on a fixed mast 6 meters from the ground. The effective isotropic radiated power (EIRP) was 17.4 dBm. The RX (receiver) was placed on a wheeled cart to facilitate its movement along the route in Fig. 4. An omnidirectional antenna with 5 dBi gain fixed at the height of 1.5 m is connected to an HP8594E Spectrum Analyzer tuned to 2.4 GHz, operating in the zero-span mode. Measurements were carried out with the TX stationary while the RX was moved throughout the living area at a speed of approximately 1.5 m/s.

Brazilian Microwave and Optoelectronics Society-SBMO received 15 Aug 2023; for review 27 Sep 2023; accepted 31 Jan 2024
Brazilian Society of Electromagnetism-SBMag *ISSN 2179-1074*

C. Wideband Measurements Setup

The wideband-sounding technique combines the advantages of the multicarrier and STDCC techniques proposed in [30], in which a PN signal modulates OFDM. The transmission setup was the same employed in narrowband channel sounding. However, a 20 MHz OFDM signal was generated in MATLAB® and transmitted by ANRITSU MG3700A Vector Signal Generator.

The reception setup included a vector signal analyzer ANRITSU MS2692A and a laptop for data recording. A PN sequence modulated the OFDM subcarriers. The signal has components in-phase (I) and quadrature (Q) and it is converted to the wave format (.wvi) used by the signal generator MG3710A via the software IQproducer®. This conversion inserts gaps of 200 null samples between symbols to ease the identification of OFDM signals in reception. The PN sequence of the OFDM signal has a length of 1023 bits, with 1 bit/sample and a sampling frequency of 50M samples/second. The transmission and reception setups used in both soundings are those shown in [30].

Typically, the PDP contains spurious peaks produced by the noise added by the channel. For accurate determination of the temporal dispersion parameters of the channel, cleanup needs to be performed to eliminate or minimize the noise effects. Previously [24], we developed an alternative technique for filtering the power delay profile using artificial neural networks to identify and extract impulsive noise. The output information from ANN will be the multipath considered valid in each PDP obtained from the field measurements. PDPs containing only valid multipath will be used to determine the channel's temporal dispersion parameters.

VII. Results and Data Analysis

The data and geographic coordinates acquired during the measurement campaigns made it possible to realize narrowband and wideband characterization.

A. Narrowband Characterization Results

For the analysis, all points of the routes were considered. In contrast, the routes were divided into small sections for small-scale analysis to check where the signal was predominantly LOS or NLOS. The received power in the narrowband varies quickly due to the fading caused by the multipath. However, according to [42], averaging power along a 20-lambda linear track (about 2.5 m for 2400 MHz) yields a reliable estimate of the average local power. From these average power values, the path loss is calculated. The path loss (PL) is defined as the ratio of the effective transmitted power to the received power, calibrating out system losses, amplifier gains, and antenna gains. The procedure adopted for determining the path loss exponent, n, from the measurements obtained in the field was developed by [43]. Fig. 5 presents a path loss scatter plot for all measurement data.

  ISSN 2179-1074

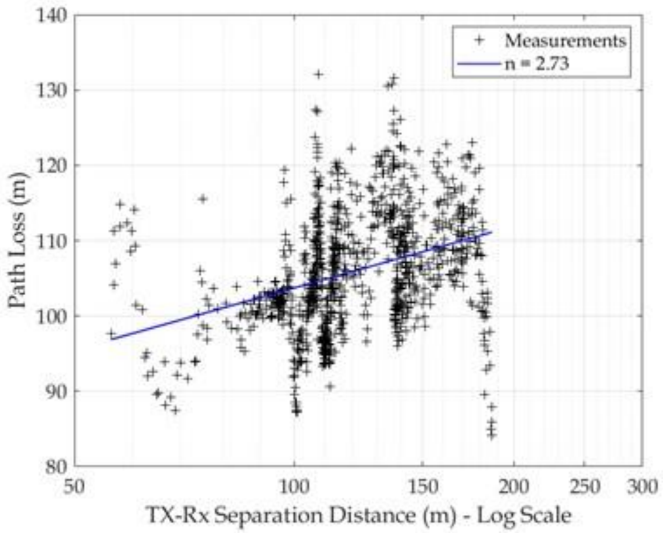

Fig. 5. Measurements and path loss adjusted to the data.

The logarithmic values of distance lead to the line of better adjustment for the path loss from which the path loss exponent, *n*, is found to be 2.73. If the transmitter antenna was higher, certainly that exponent would increase because the signal would cross the canopy of the high trees and vegetation, which is responsible for absorbing, scattering, and depolarizing the signal.

For the small-scale variability analysis, density probability function curves were drawn for the LOS and NLOS sectors, as shown in Fig. 6 (a) and Fig. 6 (b), respectively. The maximum likelihood estimates (MLEs) provide statistical parameters of Weibull, Nakagami, Rice, and Rayleigh distributions. The results showed that the Weibull and Nakagami distributions adhere better to the empirical data than the Rice and Rayleigh distributions. However, in LOS situations, the Rice distribution adheres better than the Rayleigh distribution because of the stronger direct ray. In NLOS situations, the K parameter of the Rice distribution is equal to zero, making it become Rayleigh distribution, typical of a multipath environment without sight.

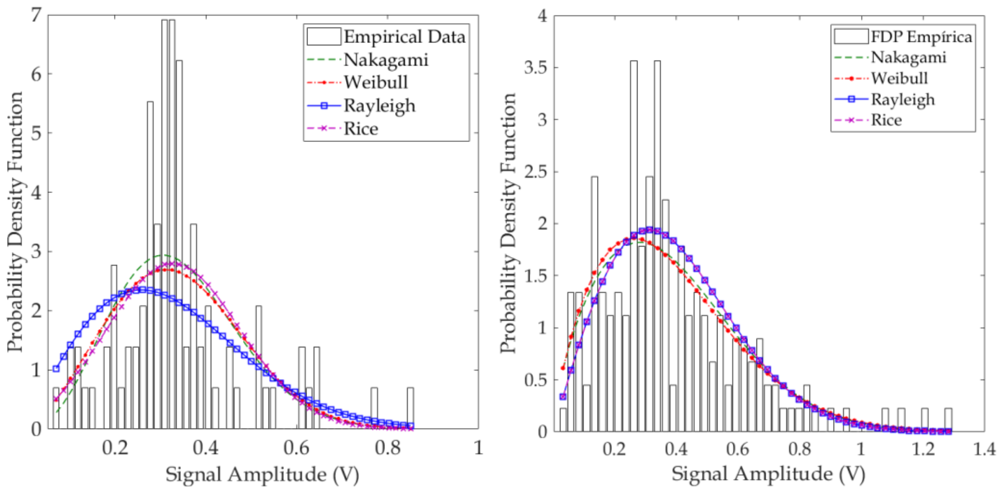

(a) (b)

Fig. 6. Small scale fading statistics (a) LOS Situation and, (b) NLOS Situation

B. Comparison with propagation loss models for environments with vegetation

Fig. 7 shows the predictions using the six specific models for vegetation environments described in Section IV.

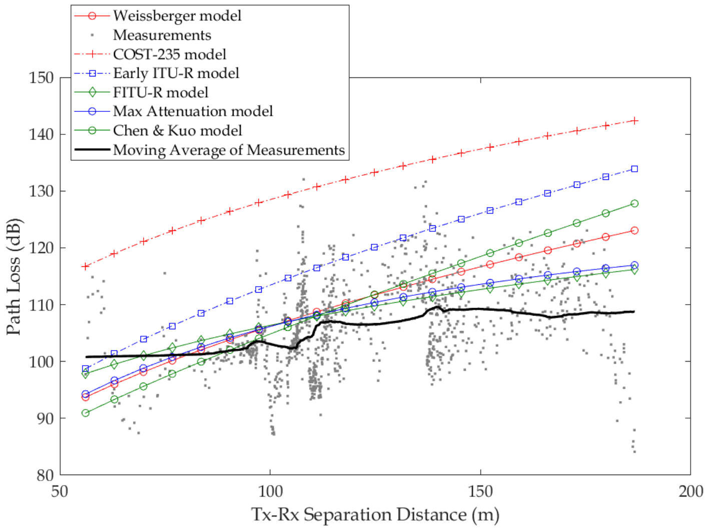

Fig. 7. Models fitted to the measurements.

A quantitative analysis through Root Mean Square Error (RMSE) between the experimental results of mean path loss and those provided by each propagation model, besides the mean absolute error (MAE), identifies the best model fitted to the data. The errors are in Table III.

TABLE III. RMS ERROR BETWEEN MODELS AND PATH LOSS RELATED TO THE DATA

Model	MAE	RMSE
Weissberger	5.20	6.07
COST 235	15.63	15.68
Early ITU-R	13.17	13.94
Fitted ITU-R	3.31	3.65
Max Attenuation	3.73	4.11
Chen and Kuo	5.54	3.94

The measurement results in the investigated environment show that the COST-235 model, and Early ITU-R model overestimate the loss propagation, providing greater losses than those found empirically. The COST-235 model was developed using a higher frequency range than the one used in this research, which justifies its high loss prediction. The Early ITU-R model proved accurate in measurements close to the transmitter. However, as the distance between Tx and Rx and the vegetation depth increases, this model presents very high prediction errors. Similar studies [44], [45], [46] also identified high prediction errors in the COST-235 and Early ITU-R models.

Weissberger, Fitted ITU-R, Chen & Kuo, and Max Attenuation models were the ones that best adhered to the empirical data. However, because they are general, their predictions would be improved with values closer to the real ones, helping to better planning in the deployment, which is the main object of our study.

The prediction improvement in the analyzed vegetated environment was performed in two parts. First, the modified exponential models, Chen & Kuo and Max Attenuation models were adjusted by nonlinear regression based on an Ordinary Least Squares (OLS) approach. Fig. 8 presents the graphical comparison of the models after the adjustment by OLS nonlinear regression for the vegetated environment.

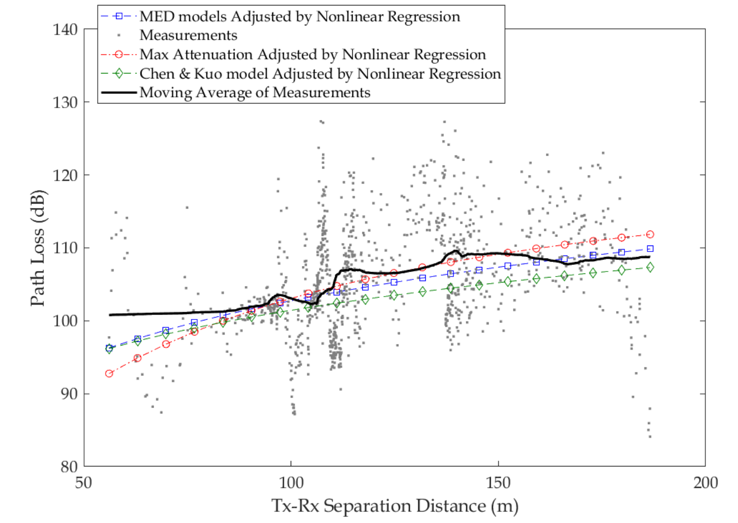

Fig. 8. Result of the models fitted by OLS nonlinear regression.

The parameters presented in (1), (2) and (3), adjusted by the OLS nonlinear regression, are shown in Table IV, and the New MAE and RMSE results after adjusting the models by OLS nonlinear regression are in Table IV. There is a significant improvement in the prediction.

TABLE IV. PARAMETERS ADJUSTED BY NONLINEAR REGRESSION

	a	b	c	d
Modified Exponential Models	0.92	0.34	0.116	-
Max Attenuation Model	1.18	0.40	-	-
Chen and Kuo Model	-0.0004	1	0.0079	1

TABLE V. PATH LOSS MODELS ERROR RESULTS AFTER ADJUSTED BY NONLINEAR REGRESSION

	MAE	RMSE
Modified Exponential Models	1.43	1.74
Max Attenuation Model	1.22	1.66
Chen and Kuo Model	5.54	3.04

Then, a nonlinear regression using artificial neural networks of the MLP type was applied. The number of input vectors and the type of variable used in the neural network are very relevant information for solving the problem. Finally, the distance between the transmitter and receiver and the path loss values, determined by the FITUR model, were used as input variables, presenting the lowest RMSE among the previously analyzed models. The database with 1070 measurement data was normalized by the Min-Max method and divided into three subsets, which are called the training subset, consisting of 60% of the total samples; the validation subset, consisting of 20% of the total samples; and a test subset, comprising 20% of the total samples set. The gradient descent and Levenberg-Marquart

ISSN 2179-1074

backpropagation algorithms were tested and the convergence time with the Levenberg-Marquart algorithm was much shorter and offered the best results in the network. According to Kolmogorov [48], in theory, only one hidden layer already offers good results for regression problems. The number of neurons in the hidden layer must maintain the compromise between overfitting and underfitting. In general, neural networks with few hidden neurons are preferred, as they tend to have better generalization power, reducing the overfitting problem. The network was tested with several numbers of hidden layers and several numbers of neurons in each hidden layer, proving to be efficient even with only one hidden layer and two neurons. No significant improvement was observed with increasing to 3 and 4 neurons in the hidden layer. The learning rate was set at 0.05 and the Levenberg-Marquart value was initially set at 10^{-3}; the goal error is 0.00001, and the epoch, which defines the number of times that the learning algorithm will work through the entire training dataset, is equal to 1000. The activation functions used were the sigmoid and linear functions for the hidden and output layers. The root mean square error was used to evaluate the network performance. The network training counted on three stopping criteria: the number of epochs, maximum permissible error value, and successive validation failures. In general, the network responded well to the configurations adopted.

Fig. 9 presents the graphic result for modeling with artificial neural networks. The MAE and RMSE values are shown in Table VI.

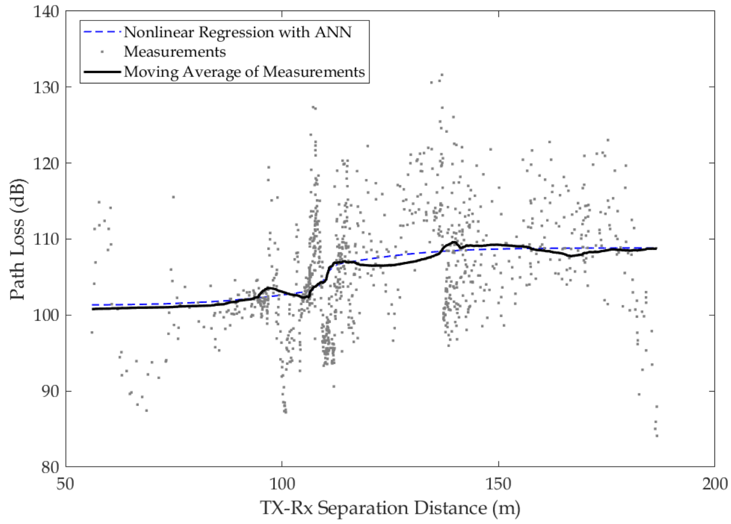

Fig. 9. Result of models fitted by ANN regression with two neurons in the hidden layer.

TABLE VI. ANN MODEL ERROR RESULTS

Number of neurons in the hidden layer	MAE	RMSE
Two	0.47	0.56
Tree	0.37	0.47
Four	0.32	0.39

The path loss prediction offered by the ANN models obtained lower MAE and RMSE results than the other models and presented better results than the OLS nonlinear regression. The nonlinear regression based on neural networks proved to be very useful in predicting the behavior of propagation losses more accurately in vegetated environments.

C. Wideband Characterization Results

After post-processing the data obtained from the wideband channel sounding, 498 PDPs were used to determine the channel's temporal dispersion parameters. The key parameters are average excess delay and RMS delay spread. Average excess delay is the average time that the replicates generated from the multipath of a signal transmitted in an instant of time (t) arrive at the receiver after the first component has reached the receiver. It is considered the first moment of the delay profile as defined at [24]-[25]:

$$\bar{\tau} = \frac{\sum_k P(\tau_k)\tau_k}{\sum_k P(\tau_k)} \tag{6}$$

in which $P(\tau_k)$ and τ_k are the amplitude and delay of each multipath that reaches the receiver.

The RMS delay spread measures the temporal spread of the delay profile around the average excess delay. The average delay spread is the square root of the second central moment of the delay profile as defined at [25]:

$$\sigma_{RMS} = \sqrt{\frac{\sum_k P(\tau_k)(\tau_k - \bar{\tau})^2}{\sum_k P(\tau_k)}} \tag{7}$$

Each of the 498 PDPs recorded 2176 samples, and the total set of available data is divided into two subsets, the training subset, consisting of 70% of the total sample, and a test subset, comprising 30% of the total sample set. The ANN training was performed after careful research on MLP network architecture. A 6-layer neural network was configurated: one input layer, four intermediate layers, and one output layer configured with 10 and 15 neurons in its layers, considering 1000 interactions.

The ANN filtering technique uses pattern recognition to identify noise and eliminate it from PDPs more effectively. The points in Fig. 10 represent the multipath components the ANN filtering technique considers true. The other delays are disregarded in calculating the average excess delay and RMS delay spread, which characterize the channel dispersion.

Fig. 10 shows a power delay profile obtained by ANN and the CFAR techniques. ANN technique found a larger number of valid multipaths compared to the CFAR technique. In [24], the authors note CFAR’s inability to resolve multipath components with shorter interarrival time. Their results show this weakness of the CFAR technique, while the ANN technique can identify these multipaths. These results show the characteristic of the ANN technique in identifying a greater number of multipath.

Brazilian Microwave and Optoelectronics Society-SBMO *received 15 Aug 2023; for review 27 Sep 2023; accepted 31 Jan 2024*
Brazilian Society of Electromagnetism-SBMag *ISSN 2179-1074*

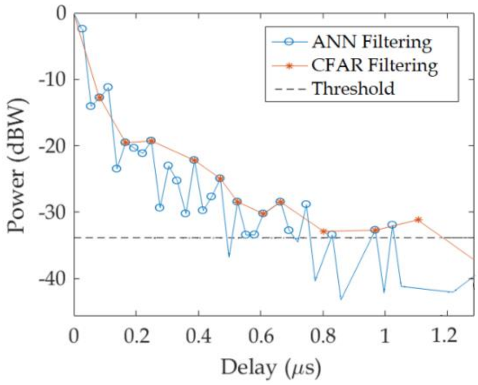

Fig. 10. ANN x CFAR Techniques Comparison.

Table VII shows the maximum and minimum values of the parameters of Average Delay and the RMS values, which are presented and do not differentiate the LOS and NLOS situations. The range of RMS delay spread found in all PDPs ranges from 32 to 301 ns, consistent with other results found in the literature in similar regions [10],[48]-[49].

TABLE VII. TEMPORAL DISPERSION PARAMETERS

	Min	**Max**	**Mean**
Average Excess Delay (ns)	3	186	58
RMS Delay Spread (ns)	32	301	121

The cumulative distributions of (a) the experimental RMS delay spread and (b) the number of multipath are shown in Fig. 11 (a) and Fig. 11 (b), respectively.

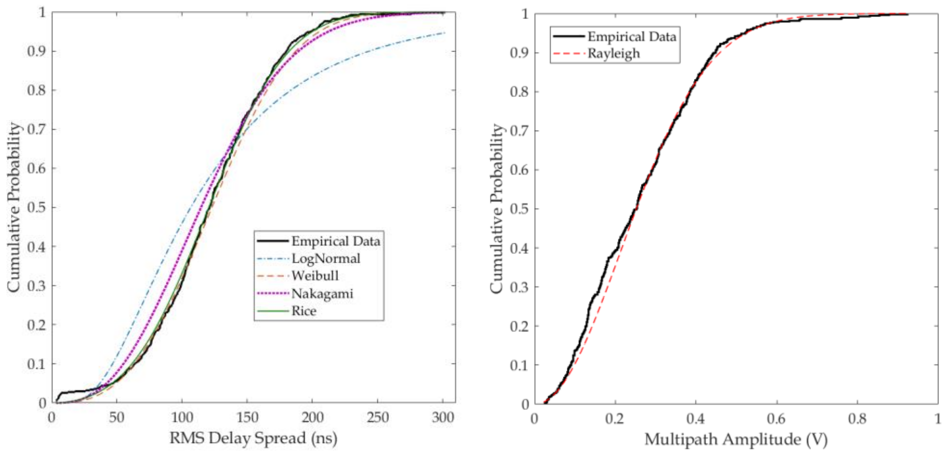

(a) (b)

Fig. 11. Cumulative distribution function of (a) the RMS delay spread and (b) the amplitude of multipath.

The Kolmogorov-Smirnov test was used to validate the adherence of the theoretical cumulative distributions with the empirical results, and the Rice distribution was the one that most adhered to both. Notably, 90% of the RMS delay spread values are below 175 ns. Besides this, the cumulative distribution of the relative amplitudes of the RMS delays showed Rayleigh-like behavior since Rayleigh is a particular case of Rice distribution when Rice K factor is null. This result is validated by the ITU-R 1411-6 recommendation [50].

Table VIII shows the RMS delay spread values obtained with other related works.

TABLE VIII. COMPARISON WITH OTHER RESULTS

Frequency	RMS Delay Spread(ns)	Reference
1.88 GHz	120	[49]
2.5 GHz	110	[10]
1.9 GHz	151	[50]

According to [51], the arrival of the multipath component follows a Poisson probability distribution in an outdoor environment, where the probability of receiving one component in the first N time intervals is given by:

$$P_N(L = l) = \frac{\lambda^l}{l!} e^{-\lambda} \tag{8}$$

and λ is the average arrival rate of the multipath components. Using the results of valid multipath components obtained after applying the ANN technique, Fig. 12 shows the fitting of the empirical results with the Poisson distribution for the number of multipath components arriving at the receiver.

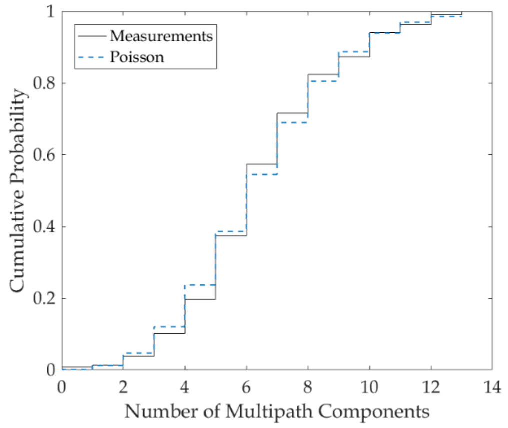

Fig. 12. Cumulative distribution function of the number of multipath.

VIII. CONCLUSIONS

This paper presents results of narrowband and wideband channel characterization from measurements in a public square with vegetation in the 2.3-2.4 GHz band.

The path loss exponent, *n*, found in the narrowband sounding was equal to 2.73. It would have a higher value if the transmitter antenna was in a position that crossed a major volume of vegetation. The path loss was compared with six specific vegetation models and sought to improve these models through two efficient regression techniques based on Ordinary Least Squares (OLS) approach and multilayer perceptron (MLP) neural networks. Although there are a variety of types of artificial neural networks, MLP-type neural networks are simple to implement and provide consistent results with minor errors.

The ITU-R model presented the best path loss prediction between the usual models, with an RMSE of 3.65 dB. Although the OLS nonlinear regression showed an improvement in the prediction capacity of the measured data in the three types of modeling analyzed (MED, Max Attenuation and Chen & Kuo), this technique does not present better results than those presented by path loss prediction models based on MLP neural networks. Different MLP neural network architectures were established and the impact of ANN architectures, the dimension and the percentage of training samples on PL prediction models was analyzed for model validation. In all cases, the RMSE was less than 0.56 dB, the architecture with one hidden layer and four neurons in each hidden layer being the one that presented the lowest RMSE value equal to 0.39 dB.

In wideband channel characterization, artificial neural networks were also used as a support tool in filtering the power delay profiles obtained from the channel impulse response. The ANN technique filtered impulsive noise, and the channel dispersion parameters were calculated. ANN technique identified other valid multipath not perceived by the CFAR technique. The RMS delay spread shows that 90% of the values are below 175 ns, using the valid multipath found by ANN. These values are fundamental in designing and planning wireless communications systems because they are mainly linked to the transmission rate permitted in a channel.

The number of multipath components that reach the receiver was also analyzed and its probability distribution adheres well to the Poisson distribution while the cumulative distribution of the relative amplitudes of the RMS delays adheres well to the Rayleigh distribution.

ACKNOWLEDGMENT

We thank the Research Support Foundation of the State of Maranhão (FAPEMA), a funding agency that fully supported the development of this work through processes UNIVERSAL-01515/16

REFERENCES

[1] P802.11ax/D8.0 - IEEE Draft Standard for Information Technology - Telecommunications and Information Exchange Between Systems Local and Metropolitan Area Networks - Specific Requirements Part 11: Wireless LAN Medium Access Control (MAC) and Physical Layer (PHY) Specifications Amendment Enhancements for High-Efficiency WLAN. https://standards.ieee.org/project/802_11 ax.html, 2020.
[2] D. Gomez-Barquero et al., "IEEE Transactions on Broadcasting Special Issue on: 5G for Broadband Multimedia Systems and Broadcasting", *IEEE Transactions on Broadcasting*, vol. 65, no. 2, pp. 351-355, 2019.
[3] S. Ozuomba, E. Johnson. “Application of Weissberger Model for Characterizing the Propagation Loss in a Gliricidia sepium Arboretum.” *Universal Journal of Communications and Network*. Vol. 6, no. 2, pp. 18 – 23, 2018.
[4] T. Jawhly, R. C. Tiwari. “Loss exponent modeling for the hilly forested region in the VHF band III,” *Radio Science*, vol. 56, no. 8, pp. 1–12, 2021.
[5] I. Picallo, H. Klaina, P. López-Iturri, E. Aguirre, M. Celaya-Echarri, L. Azpilicueta, A. Eguizábal, F. Falcone, and A. V. Alejos. “A Radio Channel Model for D2D Communications Blocked by Single Trees in Forest Environments.” *Sensors*. Switzerland, vol.19, no. 21, pp. 4606, 2019.
[6] P. Pal, R. P. Sharma, S. Tripathi, C. Kumar and D. Ramesh, "Machine Learning Regression for RF Path Loss Estimation Over Grass Vegetation in IoWSN Monitoring Infrastructure," *IEEE Transactions on Industrial Informatics*, vol. 18, no. 10, pp. 6981-6990, 2022, doi: 10.1109/TII.2022.3142318.
[7] A. S. Adewumi, O. Olabisi. “Characterization and modeling of vegetation effects on UHF propagation through a long forest channel”. *Progress In Electromagnetics Research Letters*, vol. 73, pp. 9-16, 2018.
[8] D. L. Leite, P. J. Alsina, M. M. de Medeiros Campos, V. A. de Sousa Jr, A. A. M. de Medeiros. “Unmanned Aerial Vehicle Propagation Channel over Vegetation and Lake Areas: First- and Second-Order Statistical Analysis”. *Sensors*, vol. 22, no. 1, pp. 22-65, 2022.
[9] L. Azpilicueta, P. López-Iturri, E. Aguirre, I. Mateo, J. J. Astrain, J. Villadangos, F. Falcone. “Analysis of Radio Wave Propagation for ISM 2.4 GHz Wireless Sensor Networks in Inhomogeneous Vegetation Environments”. *Sensors*, vol. 14, no. 12, pp. 23650-23672, 2014.
[10] J. C. S. Pires, L. J. Matos, L. H. Gonsioroski. “Temporal dispersion of the Mobile Radio signal in an Urban Park in the 2.5 GHz band", 16º SBMO - Brazilian Symposium on Microwave and Optoelectronics e 11º CBMag - Brazilian Congress of Electromagnetism, Curitiba, 2014.
[11] M. A. Weissberger, “An initial critical summary of models for predicting the attenuation of radio waves by trees", Electromagnetic Compatibility Analysis Center, Annapolis, Maryland, Final Report, 1982.
[12] CCIR, “Influences of terrain irregularities and vegetation on troposphere propagation", CCIR report, pp. 235-236, Geneva, 1986.

  ISSN 2179-1074

[13] COST 235, “Radio propagation effects on next generation fixed service terrestrial telecommunication systems", Final Report, Luxembourg, 1996.
[14] M. O. Al-Nuaimi, R. B. L. Stephens. “Measurement and prediction model optimization for signal attenuation in vegetation media at centimeter wave frequencies”, *IEEE Proceedings - Microwaves, Antennas and Propagations*. vol. 145. no. 3, pp. 201-206, 1998.
[15] ITU-R Rec 833-6, Attenuation in vegetation, International Telecom. Union, Geneva, 2007.
[16] H. Y. Chen, Y. Y. Kuo, “Calculation of radio Loss in Forest Environments by an Empirical Formula.” *Microwave and Optical Technology Letters*, vol. 31, no 6, pp. 474- 480, 2001.
[17] M. Haenlein and A. Kaplan, “A brief history of artificial intelligence: On the past, present, and future of artificial intelligence,” *California Manage. Rev*., vol. 61, no. 4, pp. 5–14, 2019.
[18] R. He, B. Ai, G. Wang, M. Yang, and Z. Zhong, “Wireless channel sparsity: Measurement, analysis, and exploitation in estimation,” *IEEE Wireless Communications*., vol. 28, no. 4, pp. 113–119, 2021.
[19] Q. Wu, W. Chen, C. Yu, H. Wang, and W. Hong, “Multilayer machine learning-assisted optimization-based robust design and its applications to antennas and array,” *IEEE Transactions. Antennas and Propagations*., vol. 69, no. 9, pp. 6052–6057, 2021.
[20] Y. Zhang, J. Wen, G. Yang, Z. He, J. Wang. “Path Loss Prediction Based on Machine Learning: Principle, Method, and Data Expansion”. *Applied Sciences*. vol. 9, no. 9, 2019.
[21] S. P. Sotiroudis, P. Sarigiannidis, S. K. Goudos, K. Siakavara, "Fusing Diverse Input Modalities for Path Loss Prediction: A Deep Learning Approach", *IEEE Access*, vol. 9, pp. 30441-30451, 2021, doi: 10.1109/ACCESS.2021.3059589.
[22] H.-S. Jo, C. Park, E. Lee, H. K. Choi and J. Park, "Path loss prediction based on machine learning techniques: Principal component analysis artificial neural network and Gaussian process", *Sensors*, vol. 20, no. 7, pp. 1927, 2020. https://doi.org/10.3390/s20071927
[23] N. Moraitis, L. Tsipi, D. Vouyioukas. “Performance evaluation of machine learning methods for path loss prediction in rural environment at 3.7 GHz”. *Wireless Networks*, vol. 27, pp. 4169–4188, 2021.
[24] S. Ferreira et al., "Power Delay Profile Filtering Technique Using Artificial Neural Networks," 2020 IEEE Latin-American Conference on Communications (LATINCOM), 2020.
[25] J. D. Parsons, “The Mobile Radio Propagation Channel,” John Wiley & Sons, 2nd. Ed., 2000.
[26] A. M., Guillermo. Measurements, Modeling, and OFDM Synchronization for the Wideband Mobile-to-Mobile Channel, Thesis of Ph.D., Georgia Institute of Technology, 2007.
[27] J. A. C. Bingham, “Multicarrier modulation for data transmission: An idea whose time has come,” *IEEE Communications Magazine*, vol. 28, no. 5, pp. 5–14, 1990.
[28] J. D. Parsons, D. A. Demery, and A. M. D. Turkmanil, “Sounding techniques for wideband mobile radio channels: a review”, *IEEE Proceedings Communication, speech and vision*., vol. 138, no. 5, pp. 437-446, 1991.
[29] L. H. Gonsioroski, L. A. R. Silva Mello and A. B. C. Santos, "Measurements and Modeling of the Mobile Wireless Channel at 2.4 GHz in Urban and Suburban Areas," 2021 IEEE 32nd Annual International Symposium on Personal, Indoor and Mobile Radio Communications (PIMRC), Helsinki, Finland, pp. 873-879, 2021. doi: 10.1109/PIMRC50174.2021.9569254.
[30] L. H. Gonsioroski, L. J. Matos, L. A. R. Silva Mello, C. V. R. Ron. “Characterization of a Mobile Urban Radio Channel with an Improved Multicarrier Sounding Technique," *Journal of Microwaves, Optoelectronics and Electromagnetic Applications*, vol. 14, pp. 158-167, 2015.
[31] B. J. Cavalcanti, A. G. d'Assunção, L. M. Mendonça, "Optimizing empirical propagation models for LTE and LTE-A using genetic algorithms at 879 MHz," 2017 IEEE-APS Topical Conference on Antennas and Propagation in Wireless Communications (APWC), Verona, pp. 312-315, 2017. doi: 10.1109/APWC.2017.8062313.
[32] L. Wu et al., "Artificial Neural Network Based Path Loss Prediction for Wireless Communication Network," *IEEE Access*, vol. 8, pp. 199523-199538, 2020.
[33] N. Kuno, W. Yamada, M. Inomata, M. Sasaki, Y. Asai and Y. Takatori, "Evaluation of Characteristics for NN and CNN in Path Loss Prediction," International Symposium on Antennas and Propagation (ISAP), 2021.
[34] J. Thrane, D. Zibar and H. L. Christiansen, "Model-aided deep learning method for path loss prediction in mobile communication systems at 2.6 GHz", *IEEE Access*, vol. 8, pp. 7925-7936, 2020.
[35] L. Ge e G. S. Chen, "Network structure and generalization capacity of feedforward process neural networks", *Computer Science*, vol. 35, pp. 137-150, 2008.
[36] K. Levenberg, “A method for the solution of certain problems in least squares”. *Quarterly of Applied Mathematics*. vol. 2, pp. 164–168, 1944.
[37] D. Marquardt, “An algorithm for least squares estimation of nonlinear parameters”. *Journal of the Society for Industrial and Applied Mathematics*. vol. 11, pp. 431–441, 1963.
[38] J. Y. Fan, "A Modified Levenberg-Marquardt Algorithm for Singular System of Nonlinear Equations", *Journal of Computational Mathematics*, vol. 5, pp. 625-636, 2005.
[39] L. Rosado, F. M. Janeiro, P. M. Ramos and M. Piedade, "Eddy currents testing defect characterization based on nonlinear regressions and artificial neural networks," IEEE International Instrumentation and Measurement Technology Conference Proceedings, 2012.
[40] J-L. Tang, Y-J. Liu, F-S. Wu, "Levenberg-Marquardt neural network for gear fault diagnosis," International Conference on Networking and Digital Society, 2010.
[41] E. S. Sousa; V. M. Jovanovié, C. Daigneault, “Delay Spread Measurements for the Digital Cellular Channel in Toronto”, *IEEE Transactions on Vehicular Technology*, vol. 43, pp. 837-847, 1994.
[42] W. C. Y. Lee, Mobile Cellular Telecommunications Systems, McGraw-Hill, 1990.

[43] W. Afric, B. Zovko-Cihlar, S. Grgic, “Methodology of Path Loss Calculation using Measurement Results", *IEEE Transactions on Communications*, vol. 50, pp. 495-502, 2007.
[44] J. A. Azevedo and F. E. Santos, “A model to estimate the path loss in areas with foliage of trees”. *AEU - International Journal of Electronics and Communications*, vol. 71, pp. 157–161, 2017.
[45] D. Cama-Pinto, M. Damas, J. A. Holgado-Terriza, F. Gómez-Mula, A. Cama-Pinto, “Path loss determination using linear and cubic regression inside a classic tomato greenhouse”. *International Journal of Environmental Research and Public Health*, vol. 16, no. 10, pp. 1744, 2019.
[46] A. Raheemah, N. Sabri, M. S. Salim, P. Ehkan, R. B. Ahmad, “New empirical path loss model for wireless sensor networks in mango greenhouses”. *Computers and Electronics in Agriculture*, vol. 127, pp. 553–560, 2016.
[47] A. N. Kolmogorov. “On the representation of continuous function of many variables by superpositions of continuous functions of one variable and addition”. *Doklady Akademii Nauk USSR*, vol. 114, no. 5, pp. 953–956, 1957
[48] L. J. Matos, G. L. Siqueira. “Time and Frequency Dispersion Parameters Measurements at 1.88 GHz in a Vegetated Channel”. *Journal of Communication and Information Systems (Online)*, vol. 24, pp. 24-29, 2009.
[49] C. Oestges, et al. “Radio Channel Characterization for Moderate Antenna Heights in Forest Areas”. *IEEE Transactions on Vehicular Technology*. vol. 58, no. 8, 2009.
[50] ITU-R P.1411-6, Propagation data and prediction methods for the planning of short-range outdoor radiocommunication systems and radio local area networks in the frequency range 300 MHz to 100 GHz, P Series Radiowave propagation, 2012.
[51] G. Turin, et al, “A statistical model of urban multipath propagation”. *IEEE Transactions on Vehicular Technology*, vol. 21, pp. 1-9, 1972.